Molecular Crystals and Liquid Crystals Science and Technology. Section A. Molecular Crystals and Liquid Crystals

Publication details, including instructions for authors and subscription information:
http://www.tandfonline.com/loi/gmcl19

Valence Localization and its Ordering in a Mixed-Valence MMX-Chain Complex, $Pt_2(dta)_4I$ ($dta = CH_3CS_2^-$)

Hiroshi Kitagawa [a], Noriaki Onodera [a] & Tadaoki Mitani [a]

[a] School of Materials Science, Japan Advanced Institute of Science & Technology, Tatsunokuchi, Ishikawa, 923-1292, Japan

Version of record first published: 24 Sep 2006

To cite this article: Hiroshi Kitagawa, Noriaki Onodera & Tadaoki Mitani (2000): Valence Localization and its Ordering in a Mixed-Valence MMX-Chain Complex, $Pt_2(dta)_4I$ ($dta = CH_3CS_2^-$), Molecular Crystals and Liquid Crystals Science and Technology. Section A. Molecular Crystals and Liquid Crystals, 342:1, 111-120

To link to this article: http://dx.doi.org/10.1080/10587250008038253

Mol. Cryst. Liq. Cryst., 2000, Vol. 342, pp. 111-120
Reprints available directly from the publisher
Photocopying permitted by license only

Valence Localization and its Ordering in a Mixed-Valence MMX-Chain Complex, $Pt_2(dta)_4I$ ($dta = CH_3CS_2^-$)

HIROSHI KITAGAWA, NORIAKI ONODERA and TADAOKI MITANI

School of Materials Science, Japan Advanced Institute of Science & Technology, Tatsunokuchi, Ishikawa 923–1292, Japan

The temperature dependencies of UV-VIS-NIR, IR, and Raman spectra of an MMX-type halogen-bridged mixed-valence complex $Pt_2(dta)_4I$ ($dta = CH_3CS_2^-$) and the monovalent dimers $Pt_2(dta)_4$ and $Pt_2(dta)_4I_2$ were investigated. The former undergoes a metal-insulator transition at 300 K, below which a characteristic splitting of C=S stretching mode was observed. The valence localization and its ordering are considered to occur coupled to the metal-insulator transition; $-Pt^{2.5+}$-$Pt^{2.5+}$–I–$Pt^{2.5+}$-$Pt^{2.5+}$–I– is for the metallic phase, while $-Pt^{2+}$-Pt^{3+}-I–Pt^{2+}-Pt^{3+}-I– for the insulating one.

Keywords: MX chain; mixed valency; charge ordering; molecular conductor; mott transition; valence instability

INTRODUCTION

In a pure one-dimensional (1-D) electronic system, several kinds of fluctuations, such as spin, charge, orbital, lattice, *etc.*, can play an essential role. In practice, these are frozen due to weak three-dimensional interactions. Consequently, various kinds of ordered phases are formed according to the type of interactions. If the internal degrees of freedom of 1-D electronic

system could be increased, it may be possible to revive the frozen fluctuations.

In recent years, halogen-bridged 1-D transition-metal complexes (MX chains) have been intensively investigated from viewpoints of physics and chemistry as a model of 1-D electronic system [1-3]. The MX chains have been regarded as 1-D metal in which a half-filled conduction band is made up primarily of an antibonding combination of the transition metal M d_{z^2} orbitals and the bridging halogen X p_z orbitals. In reality, all of the MX chains synthesized until now are insulating, which means a freezing of charge degree of freedom.

In this work, we have focused on a spin-charge-lattice strongly coupled system latently having valence instability. In this system 1-D ···-M-M-X-M-M-X-··· neutral chains are formed (called MMX-chain) [4-11], in which a new degree of freedom, charge (valence) polarization, is introduced to the M-M dimeric unit. The formal valence state of the metal is +2.5, which means an M-M dimeric unit has one spin. According to our recent work [12-15], the title complex was found to exhibit metallic above 300 K. Due to direct overlap of the M(d_{z^2})-M(d_{z^2}) orbitals, the width of the conduction band and the on-site Coulomb repulsion U become wider and decreased in MMX chains, respectively, than in MX chains. At 300 K (= $T_{M\text{-}I}$), it undergoes a metal-semiconductor transition, which is considered to be of Mott-type with charge ordering of $-Pt^{2+}$-Pt^{3+}-I-Pt^{2+}-Pt^{3+}-I–. Below 90 K, it also shows a magnetic anomaly and insulating behavior, which may be a spin-Peierls-like state with alternate charge ordering of $-Pt^{2+}$-Pt^{3+}-I-Pt^{3+}-Pt^{2+}–I–. In order to understand the valence localization at $T_{M\text{-}I}$ and the valence ordering states below $T_{M\text{-}I}$, we have measured the temperature dependencies of the VIS-UV-NIR, IR, and Raman.

EXPERIMENTAL

The monovalent and mixed-valence complexes were prepared by the method previously reported [4, 6]. Single crystals were obtained by two different methods; one is a recrystallization method cooling slowly from hot toluene solutions containing the mixture of $Pt_2(dta)_4$ and I_2, the other is

a slow diffusion method at room temperature (r.t.) in an H-tube cell containing $Pt_2(dta)_4$ and I_2 in each of the sides. The quality of the single crystals was checked by X-ray single-crystal analysis, elemental analysis, and IR spectroscopy.

For optical absorption spectra, powdered samples ground down from single crystals were diluted with KBr and then the mixtures were processed into pellets under pressure (~ 6 Kbar) and vacuum condition. The UV-VIS-NIR absorption spectra were measured in the temperature range 1.6 - 425 K by use of a Jasco V-570 spectrometer with an OXFORD Optistat^{CF} cryostat. IR spectra were measured in the temperature region of 11 – 475 K by a Nicolet FTIR 800 spectrometer with a DAIKIN CryoKelvin 202CL cryostat that possesses KRS-5 optical windows. IR detectors of TGS and MCT were used.

Polarized Raman spectra of single crystals were measured with a Jasco NR-1800 subtractive-dispersion triple polychromator using a microscope. A Spectra-Physics model 2017 Ar^+ laser provided the exciting line (514.5 nm). Detection of the scattered radiation was made by a cooled Photometrics CC200 CCD camera system with operating temperature of 153 K. Laser power at the crystal was held to < 0.1 mW to avoid laser damage to samples. In order to reduce stray light from Rayleigh scattering and enable low-frequency Raman spectroscopy down to 20 cm^{-1}, the positions of double subtractive premonochromator and third monochromator were shifted to each other by 50 cm^{-1} and the Rayleigh light was cut by a slit between the first and second monochromators. Wavenumber calibration was effected by reference to the emissions of Ne lamp. The typical dimension of flat needle-like crystal was *ca.* 2 x 0.4 x 0.1 mm. The $Z(YY)\overline{Z}$ and $Z(XX)\overline{Z}$ components of the scattered radiation were used, where X // c^*, Y // b^*, Z // a^*-c^* (~ a), and the 1-D chain // b^* (=b)

RESULTS AND DISCUSSIONS

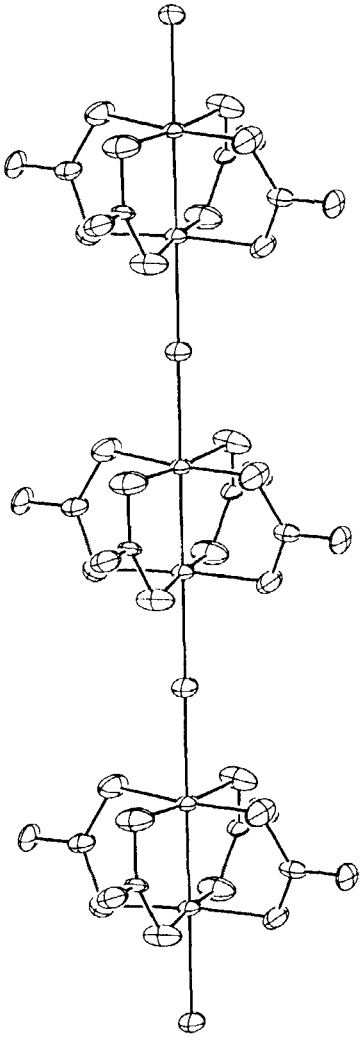

FIGURE 1 1-D chain structure of the title MMX-Chain complex of at r.t.

Figure 1 shows the 1-D chain structure of the MMX chain $Pt_2(dta)_4I$ at r.t. The MMX chain is a binuclear unit-assembled system containing metal-metal bonds, so that there exists an internal degree of freedom of charge polarization in dimer units. Therefore, a wide variety of possible electronic structures are considered for the MMX system. Some of the possible 1-D charge-ordering states for this chain system are shown as below.

(1) $-Pt^{2.5+}$-$Pt^{2.5+}$–I–$Pt^{2.5+}$-$Pt^{2.5+}$–I–
(2) $-Pt^{2+}$-Pt^{2+}–I-Pt^{3+}-Pt^{3+}-I–
(3) $-Pt^{2+}$-Pt^{3+}-I–Pt^{2+}-Pt^{3+}-I–
(4) $-Pt^{2+}$-Pt^{3+}-I-Pt^{3+}-Pt^{2+}–I–

The mode (1) is an average charge ordering state, (2) is a charge-density-wave(CDW) state, (3) is a charge-polarization state, and (4) is alternate charge-polarization state similar to spin-Peierls distortions.

Figure 2 shows the absorption spectra of the mixed-valence complex $Pt^{II}Pt^{III}(dta)_4I$, and the monovalent complexes $Pt^{II}Pt^{II}(dta)_4$ and $Pt^{III}Pt^{III}(dta)_4I_2$. The strong broad band observed at 0.9 eV for $Pt_2(dta)_4I$ is assigned to the inter-

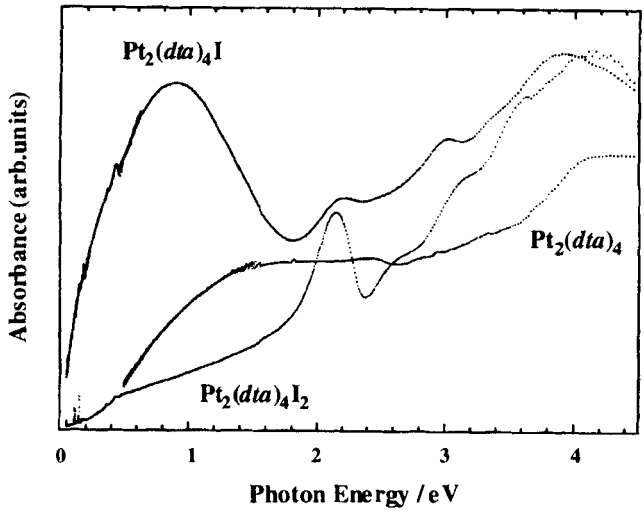

FIGURE 2 Absorption spectra for mixed-valent $Pt_2(dta)_4I$ and monovalent $Pt_2(dta)_4$ and $Pt_2(dta)_4I_2$ at r.t.

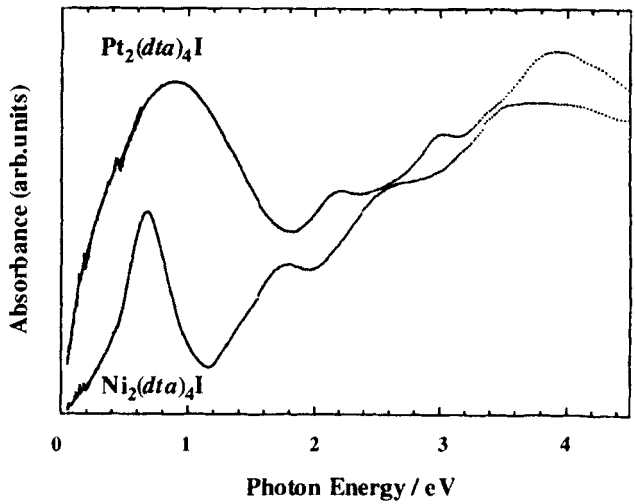

FIGURE 3 Absorption spectra of $Ni_2(dta)_4I$ and $Pt_2(dta)_4I$ at r.t.

dimer charge transfer from the electronic configuration of $d_\sigma^2 d_{\sigma^*}^1$, $d_\sigma^2 d_{\sigma^*}^1$ to that of d_σ^2, $d_\sigma^2 d_{\sigma^*}^2$. The dominant absorption features at higher-energy side are two bands centered at 2.2 eV and 3.0 eV, which are attributable to the ligand-to-metal charge-transfer (LMCT; $I(p_\sigma) \rightarrow Pt(d_{\sigma^*})$) and the intradimer ($d_{\pi^*} \rightarrow d_{\sigma^*}$) transitions, respectively. The two bands are also observed for oxidized $Pt_2(dta)_4I_2$ of which the d_{σ^*} orbital is unoccupied, and both are not observed for the reduced species $Pt_2(dta)_4$ when d_{σ^*} is fully occupied [4, 5]. The former band is shifted to higher-energy side in the order of $Pt_2(dta)_4I_2$ (2.2 eV) < $Pt_2(dta)_4Br_2$ (2.5 eV) < $Pt_2(dta)_4Cl_2$ (2.7 eV), while the energy of the latter band is almost unchanged [4]. These facts are consistent with the above assignments.

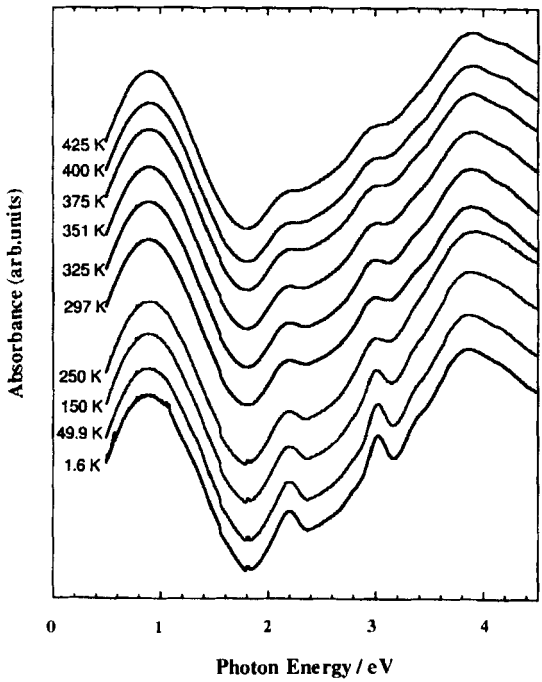

FIGURE 4 Temperature dependence of the UV-VIS-NIR absorption spectra for $Pt_2(dta)_4I$.

Figure 3 shows the absorption spectra of $Ni_2(dta)_4I$ and $Pt_2(dta)_4I$. The interdimer charge transfer band from the electronic configuration of $d_\sigma^2 d_{\sigma^*}^1$, $d_\sigma^2 d_{\sigma^*}^1$ to that of d_σ^2, $d_\sigma^2 d_{\sigma^*}^2$ was observed at 0.65 eV that is attributed to a Mott-Hubbard splitting at the Fermi energy. The ligand-to-metal charge-transfer $I(p_\sigma) \rightarrow M(d_\sigma^*)$ and the intradimer $(d_\pi^* \rightarrow d_\sigma^*)$ transitions are shifted to the lower-energy side in $Ni_2(dta)_4I$, which are due to the lower-energy level of Ni(3*d*) and smaller Ni(3*d*)-Ni(3*d*) overlapping, respectively, than those of Pt(5*d*).

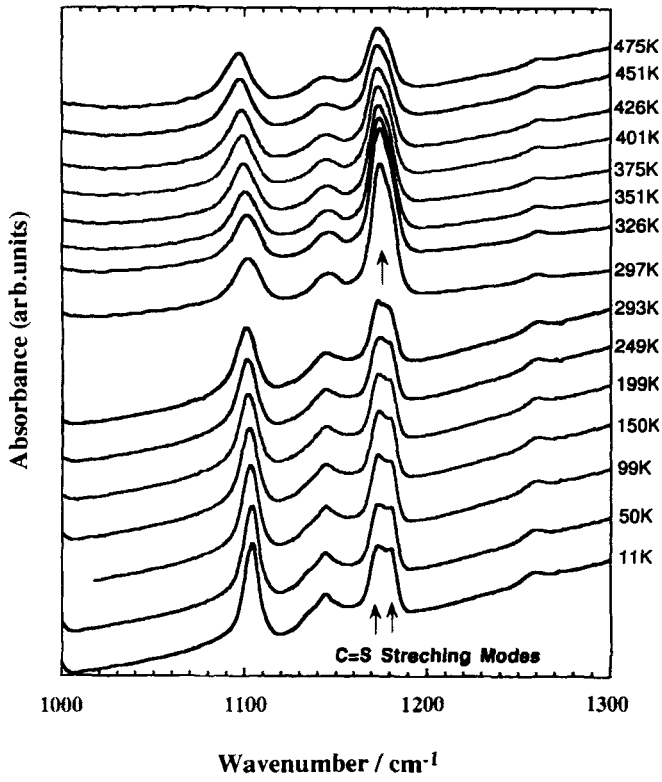

FIGURE 5 Temperature dependence of IR absorption in the C=S stretching region.

Figure 4 shows the temperature dependence of UV-VIS-NIR absorption spectra for $Pt_2(dta)_4I$. No noticeable change or energy shift was observed at all temperatures except for band narrowing at low temperature. IR absorption spectra, on the other hand, showed a characteristic splitting of C=S stretching mode at 1180 cm^{-1} below T_{M-I}, as shown in Figures 5 and 6. This mode is quite sensitive and reflects the charge polarization state of the intermetallic Pt-Pt bond in the $[Pt_2(dta)_4]$ unit. The single peak observed above T_{M-I} strongly suggests that the electronic state is in the uniform charge distribution, that is mode (1). On the other hand, the two peaks observed below T_{M-I} show a localized-valence state of Pt^{2+} and Pt^{3+}.

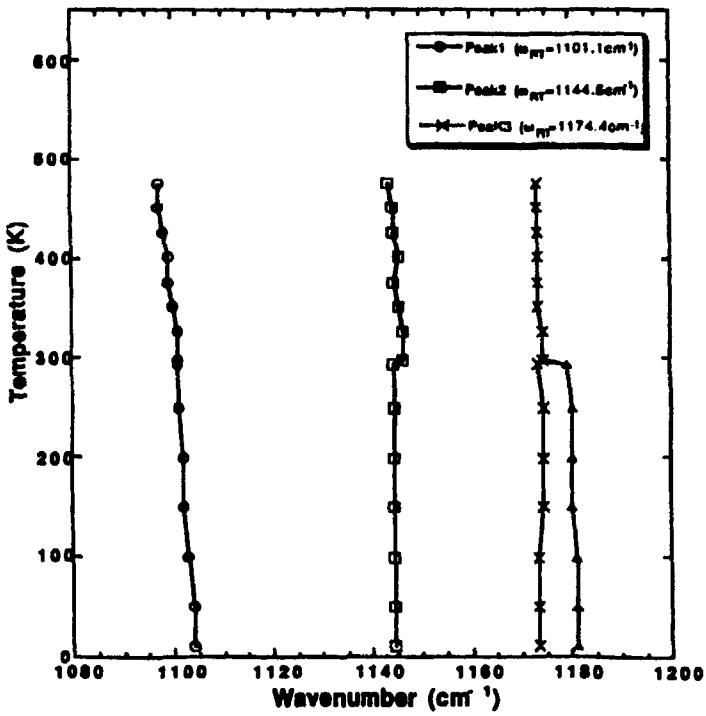

FIGURE 6 Temperature dependence of frequencies of the IR modes in the energy region of 1080 – 1200 cm^{-1}.

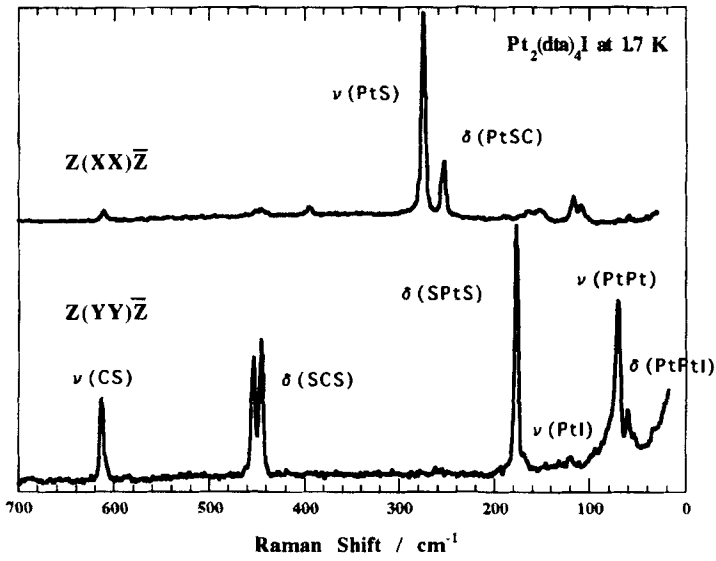

FIGURE 7 Polarized Raman spectra of $Pt_2(dta)_4I$ at 1.7 K.

This is evidence of valence transition from an average-valence state to a valence-trapped state at $T_{M\text{-}I}$. So one of the modes (2)-(4) can be responsible for the semiconducting state. We reported that the semiconducting state still has a spin degree of freedom, that is a Mott insulator [15]. Accordingly, the mode (3) is more favorable for the semiconducting state.

As can be seen in Figure 7, very weak ν(Pt-I) mode at 120 cm^{-1} and no overtones were observed for the polarization of $Z(YY)\overline{Z}$ in $Pt_2(dta)_4I$. The iodine ions could be centrally bridging between the $Pt_2(dta)_4$ units, otherwise the ν(Pt-I) mode would be strongly Raman-active. The other important mode, which is assigned to Pt-Pt stretching mode (70 cm^{-1}), is a singlet. So the chain structure of the metallic state can be interpreted in terms of either model of the mode (1) or (4) from the Raman study. The ν(Pt-Pt) and ν(Pt-I) modes are strongly y-polarized, which reflects a 1-D electron-lattice coupled system.

In summary, we have studied optical properties of $Pt_2(dta)_4I$. The valence localization and its ordering are found to occur below $T_{M\text{-}I}$.

Acknowledgments

This work was partly supported by Grand-in-Aid Scientific Researches No. 11640559 and No. 401 of Priority Areas (Metal-Assembled Complexes) from the Ministry of Education, Science, Sports and Culture, Japan, and by the Izumi Science and Technology Foundation.

References

[1] H. J. Keller, in *Extended Linear Chain Compounds*, edited by J. S. Miller, (Plenum, New York, 1982), **Vol.1,** p.357.
[2] P. Day, in *Low-Dimensional Cooperative Phenomena*, edited by H. J. Keller, (Plenum, New York, 1974), p.191.
[3] R. J. H. Clark, in *Mixed Valence Compounds*, edited by D. E. Brown, (Reidel, Dordrecht, 1982), p.271.
[4] C. Bellitto, A. Flamini, L. Gastaldi, L. Scaramuzza, *Inorg. Chem.*, **22**, 444 (1983).
[5] C. Bellitto, G. Dessy, V. Fares, *Inorg. Chem.*, **24**, 2815 (1985).
[6] C. Bellitto, A. Flamini, O. Piovesana, P. F. Zanazzi, *Inorg. Chem.*, **19**, 3632 (1980).
[7] M.-H. Whangbo, E. Canadell, *Inorg. Chem.*, **25**, 1727 (1986).
[8] R. J. H. Clark, J. R. Walton, *Inorg. Chem. Acta*, **129**, 163 (1987).
[9] S. Kinoshita, H. Wakita, M. Yamashita, *J. Chem. Soc. Dalton Trans.*, 2457 (1989).
[10] M. Yamashita, Y. Wada, K. Toriumi, T. Mitani, *Mol. Cryst. Liq. Cryst.*, **216**, 207 (1992).
[11] R. Ikeda, N. Kimura, H. Ohki, T. Furuta, M. Yamashita, *Synthetic Metals*, **71**, 1907 (1995).
[12] H. Kitagawa, N. Onodera, J.-S. Ahn, T. Mitani, K. Toriumi, M. Yamashita, *Mol. Cryst. Liq. Cryst.*, **285**, 311 (1996).
[13] H. Kitagawa, N. Onodera, T. Mitani, K. Toriumi, M. Yamashita, *Synthetic Metals*, **86,** 193 (1997).
[14] H. Kitagawa and T. Mitani, *Coord. Chem. Rev.*, **190–192,** 1169–1184 (1999).
[15] H. Kitagawa, N. Onodera, T. Sonoyama, M. Yamamoto, T. Fukawa, T. Mitani, M. Seto, Y. Maeda, *J. Am. Chem. Soc.*, **121,** 10068–10080 (1999).